Chemistry–A European Journal
Research Article
doi.org/10.1002/chem.202401771
Chemistry Europe
European Chemical Societies Publishing
www.chemeurj.org

A Macrocyclic Tweezers-Shaped Receptor for the Biomimetic Recognition of the Gal(α1-3)Gal Disaccharide of the α-Gal Antigen

Francesco Milanesi,[a] Nastassja Burrini,[a] Giona Corti,[a] Stefano Roelens,[b] and Oscar Francesconi*[a]

The Gal(α1-3)Gal is the terminal disaccharide unit of the α-Gal epitope [Gal(α1-3)Gal(β1-4)GlcNAc], an exogenous antigenic determinant with several clinical implications, found in all non-primate mammals and in several dangerous pathogens, including certain protozoa and mycobacteria. Its absence in humans makes the α-Gal epitope an interesting target for several infectious diseases. Here we present the development of a macrocyclic tweezers-shaped receptor, resulting from the combination of the structural features of two predecessors belonging to the family of diaminocarbazole receptors, which exhibits binding properties in the low millimolar range toward the Gal(α1-3)Gal disaccharide of the α-Gal antigen.

Introduction

Exposed on the surface of eukaryotic cells as glycoconjugates of lipids and proteins, glycans mediate a variety of events in cell-cell, cell-matrix and cell-molecule interactions, including those related to the regulation of the immune response.[1,2] The complexity of glycan structures determines their biological role, in such a way that selective recognition of specific terminal epitopes by the immune system determines the discrimination of self from non-self.[3] Molecular recognition is the key step in these processes, thus development of synthetic receptors capable of recognising oligosaccharide epitopes and of interfering with these events has gained increasing interest in the last few years.[4,5]

Among the plethora of biologically relevant oligosaccharides, the α-Gal epitope [Gal(α1-3)Gal(β1-4)GlcNAc] has unique clinical relevance.[6] Indeed, it is abundantly expressed as a terminal on glycoconjugates of non-primate mammals, prosimians, and New World monkeys, whereas it is not expressed in apes, Old World monkeys and humans; rather, the latter produce an anti-Gal antibody that specifically binds to the α-Gal epitope. This is one of the major obstacles to xenotransplantation[7] and the origin of the alpha-gal syndrome,[8] a meat allergy onsetting after the bite of certain ticks, whose saliva is an α-Gal-containing antigen, that induces the immune system to release specific IgE. In addition, the α-Gal epitope is also expressed on the surface of several pathogens of high risk to human health,[9] such as various species of protozoa and mycobacteria, and is proven to be a specific target for the treatment of infectious diseases, such as leishmaniasis,[10] malaria, and tuberculosis.[11]

Following a biomimetic approach, based exclusively on non-covalent interactions, the investigation of synthetic receptors for carbohydrates has long been restricted to organic solvents, where polar interactions are enhanced by the mild competition of solvent molecules.[12] Indeed, water poses a serious obstacle to the recognition of polar species such as carbohydrates,[13–15] and biomimetic receptors effective in water have only recently been on the rise in the literature.[4,16] While the use of "temple" architectures has given good results in terms of affinity and selectivity in water toward all-equatorial carbohydrates like glucose,[17,18] there are few examples in the literature of receptors capable of recognizing in water biologically relevant mono- and oligosaccharides with axial substituents and/or α-glycosidic linkages.[19–22] Although D-glucose (Glc) is of central interest for the development of sensors monitoring glucose levels in biological fluids,[23] monosaccharides other than Glc are far more common as terminal epitopes in glycans,[24] such as D-galactose (Gal), L-fucose (Fuc), D-mannose (Man), N-acetyl-D-glucosamine (GlcNAc), N-acetyl-D-galactosamine (GalNAc), and N-acetylneuraminic acid (Neu5Ac).

Recently, our research group has developed a family of biomimetic receptors based on diaminocarbazole as hydrogen bonding unit, noticeably effective toward carbohydrates in water.[25] A macrocyclic member of this family (**1**, Figure 1),[22] which is constituted of alternated 9,10-disubstituted anthracene and diaminocarbazole units, shows interesting recognition properties toward axially substituted monosaccharides, such as the methyl glycosides of α-glucose (MeαGlc), α-galactose

[a] Dr. F. Milanesi, N. Burrini, G. Corti, Prof. O. Francesconi
Department of Chemistry "Ugo Schiff", DICUS
Università degli Studi di Firenze
Campus Sesto, 50019 Sesto Fiorentino, Firenze (Italy)
E-mail: oscar.francesconi@unifi.it
[b] Dr. S. Roelens
Consorzio Interuniversitario Nazionale per la Scienza e Tecnologia dei Materiali (INSTM)
Department of Chemistry "Ugo Schiff", DICUS
Campus Sesto, 50019 Sesto Fiorentino, Firenze (Italy)

Supporting information for this article is available on the WWW under https://doi.org/10.1002/chem.202401771

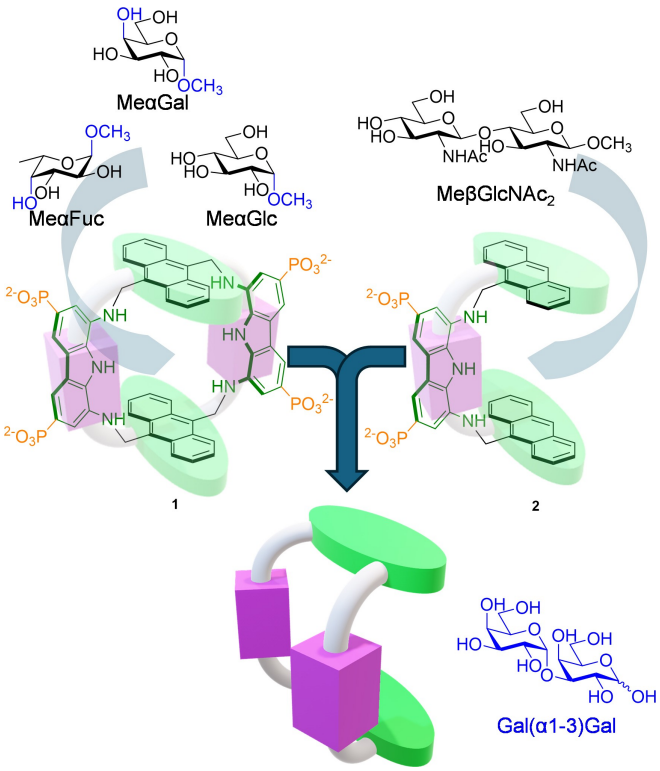

Figure 1. Schematic representation of the strategy followed to combine the macrocyclic architecture of **1** with the tweezers-like shape of **2** in a new binding architecture. Glycosides targeted by receptors **1** and **2**, and structure of the Gal(α1–3)Gal disaccharide of the α-Gal antigen, are also depicted in the figure.

(MeαGal) and α-fucose (MeαFuc) in water. The selectivity of macrocyclic receptor **1** is mainly directed to 1,4-diaxially-substituted monosaccharides, such as MeαGal and MeαFuc, based on an extended hydrogen bonding network established with the two diaminocarbazole units. Despite the interesting results obtained with monosaccharides, **1** shows only moderate binding abilities toward disaccharides, mainly because of the size of the macrocyclic cavity.[26] Conversely, a homologous member of the family (**2**, Figure 1),[27,28] which shows a tweezers-like shape and a single diaminocarbazole hydrogen-bonding unit in an open-chain architecture, does not bind to monosaccharides, but exhibits peculiar recognition properties toward disaccharides, in particular toward the *N,N'*-diacetylchitobiose (βGlcNAc$_2$), even when this is present in the core structure of N-glycans.

Here we present the design and the synthesis of a new member of the diaminocarbazole family which, taking advantage of the structural features of previous receptors, combines the macrocyclic architecture of **1** with the tweezers-like shape of **2**, to realize a receptor capable of recognizing both, axially substituted monosaccharides, such as MeαGal, and disaccharides, such as the Gal(α1-3)Gal unit of the α-Gal antigen.

Results and Discussion

Encouraged by the affinity in the low millimolar range of receptor **1** toward MeαGal, we initially investigated the recognition of the Gal(α1-3)Gal disaccharide using this architecture. A ^{1}H-NMR titration of Gal(α1-3)GalβOMe, which is structurally related to the α-Gal epitope, with **1** was carried out in D$_2$O at pD 7.4, 298 K. Setting the independently measured dimerization constant of receptor **1** at pD 7.4 ($\log\beta_{dim} = 3.84 \pm 0.20$)[22] as invariant in the non-linear regression analysis, a model in which a receptor-glycoside complex showing exclusively a 2:1 (R:G) stoichiometry was found, featuring a $\log\beta_{(2:1)} = 6.22 \pm 0.01$. Because both dimerization and binding constants were observed in the equilibrium system, the affinity was assessed using the intrinsic median binding concentration parameter BC_{50}^0,[29] resulting in an affinity value of $BC_{50}^0 = 9.18 \pm 0.25$ mM. In contrast, when an equimolar amount of Gal(α1-3)GalβOMe was added to the acyclic receptor **2**, no significant chemical shift variation was detected (Figure S8), indicating a negligible binding. Following the idea that a synergistic combination of a macrocyclic structure, with two diaminocarbazole hydrogen bonding units oriented inward the cavity, with a tweezers-like architecture, featuring an adaptive binding cleft, might improve the binding ability toward a complex structure such as that of Gal(α1-3)GalβOMe, we designed receptor **3** (Scheme 1). Due to the 2,7-disubstitution of the naphthalene ring, receptor **3** can adopt a tweezers-like conformation, as suggested by molecular modelling calculations (Figure S28).

Receptor **3** was easily synthesized in three steps with 54% overall yield starting from two readily available building blocks, 2,7-naphthalenedicarboxaldehyde (**4**)[30] and diaminocarbazole (**5**),[22] prepared according to previously described procedures. Macrocyclization was carried out in a one-pot reaction, using an equimolar mixture of **4** and **5** in $CHCl_3$, which was refluxed overnight before $NaBH_4$ in methanol was added to reduce the

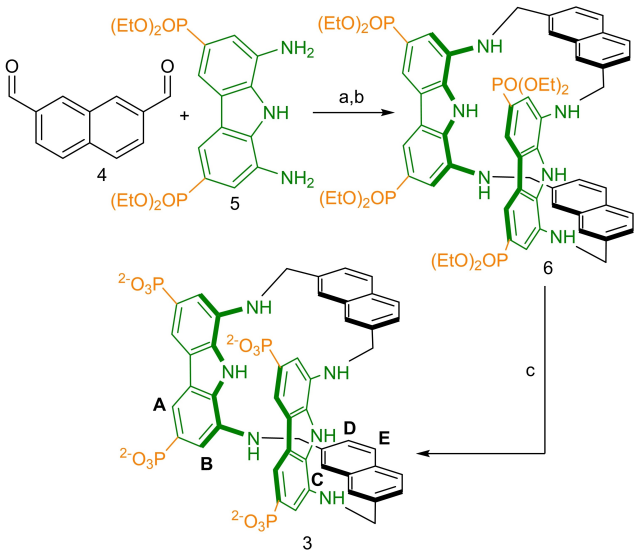

Scheme 1. Synthesis of receptor **3**. Reagents and conditions: (a) $CHCl_3$, reflux, 18 h; (b) $NaBH_4$, MeOH/$CHCl_3$, RT, 4 h (60% yield over 2 step); (c) TMSBr, Et_3N, DCM, RT, 16 h, then MeOH, 0.5 h, RT (90% yield).

formed imines, affording the tetraamine **6** in 60% yield. Hydrolysis of the phosphonate esters was carried out using trimethylbromosilane, followed by methanol, to give the hydrosoluble receptor **3** with a 90% yield over two steps.

Structure Studies of the Receptor

Receptor **3** was freely soluble in water over a wide range of pH, from physiological (pH 7.4) to alkaline (pH 11), whereas it precipitated under acidic conditions, due to the high degree of protonation of the phosphonate groups. The ^{1}H-NMR spectra of receptor **3** recorded at different pH values showed significant differences when moving from pH 11, where phosphonates are completely deprotonated, to pH 7.4, where partial protonation is occurring (Figure 2a). Indeed, whereas at pH 11 a set of sharp signals was observed, at pH 7.4 the signal of the H–C proton of the naphthalene ring was dramatically broadened and upfield shifted by a $\Delta\delta$ of 1.8 ppm, lying in a spectral region quite distant from that of other aromatic protons. Similarly, the CH_2 signal shifted upfield and broadened, apparently affected by the same phenomena. A stepwise variation of pH from 11 to 5 (Figure S9) showed that the ^{1}H-NMR signals remained relatively unperturbed down to pH 9, then showed a gradual shift, broadening, and disappearance of the H–C and CH_2 protons; this behavior suggests a fast exchange process in the NMR time scale, strictly related to the degree of protonation of the phosphonate groups. Dilution experiments on receptor **3** at pH 7.4 in D_2O fitted a self-association model where a trimer was the only species observed. The strong trimerisation constant measured ($\log\beta_{trim} = 6.71 \pm 0.06$) makes the trimer as the main species in solution at low millimolar concentrations. As an independent experimental evidence, the presence of a trimeric species was also supported by MALDI-MS experiments (see Figures S6, S7). The observation that the H–C and CH_2 protons shift upfield, both when concentration increases and when pH decreases, suggests that the strong perturbation affecting the two signals is related to an increase in the mole fraction of the trimeric species, whereby these protons most likely are affected by an intermolecular shielding effect caused by the aromatic rings. In addition, dilution experiment on receptor **3** at pH 11 does not show any self-association phenomena (no variation in chemical shifts was observed, see Figure S13); this evidence indicates that self-association, which in these systems is usually caused by π-stacking interactions,[31] is here most probably driven by hydrogen bond formation between partially protonated phosphonate groups. NOESY spectra were thus carried out on receptor **3** at both, pH 7.4 (Figure 2b) and pH 11 (Figure S24–25). At pH 7.4 the NOESY spectrum showed NOE cross-peaks of the methylene bridges with the H–D protons of naphthalene and with the H–B protons of carbazole. Moreover, an NOE contact was detected between H–C and H–B. Because these NOEs were also found at pH 11, they were assigned to intramolecular contacts within the monomeric **3**. Curiously, another NOE cross-peak was found at pH 7.4, but not at pH 11, between the H–C and H–D protons of the naphthalene,

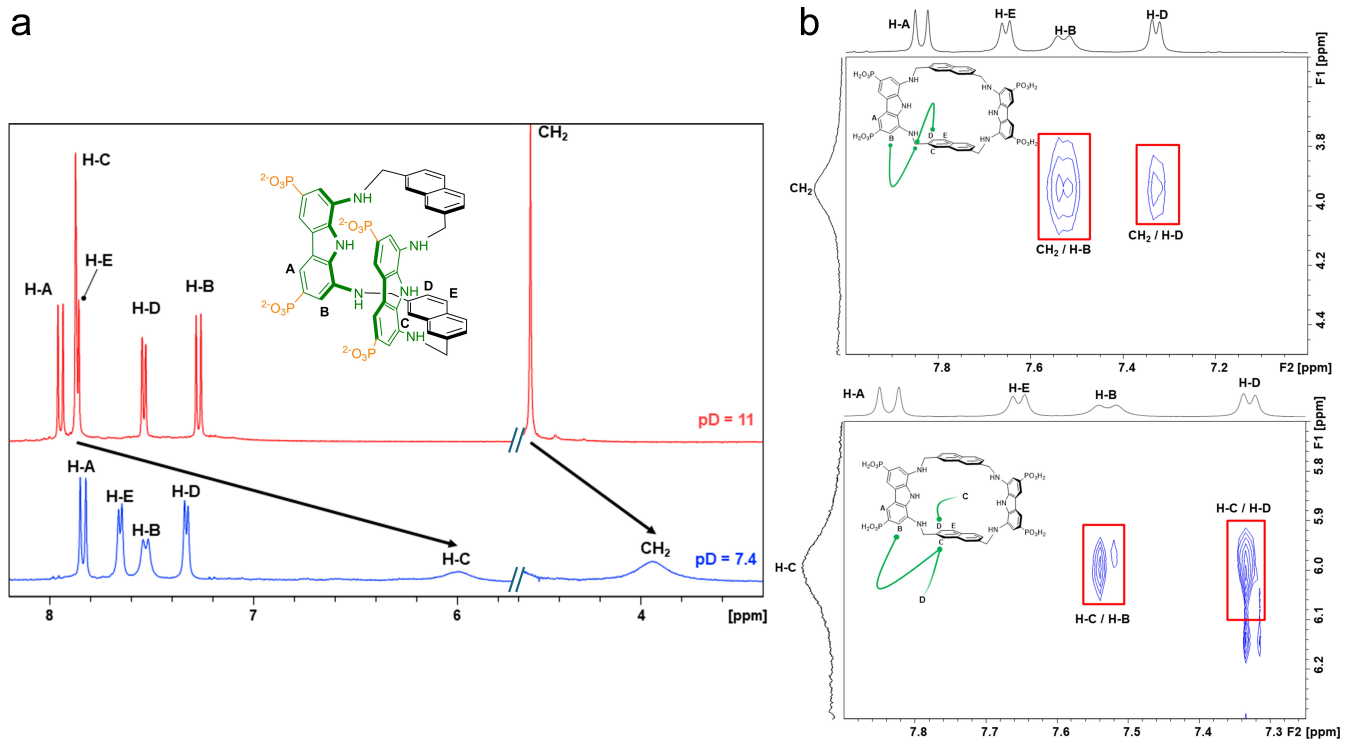

Figure 2. NMR self-association studies: a) ^{1}H-NMR spectra (500 MHz, 298 K) of receptor **3** (7 mM) at two different pD values, 11 (top) and 7.4 (bottom). Proton signals are labelled and variation of chemical shifts of protons H–C and CH_2 are indicated with arrows; b) NOESY (300 ms mixing time, 500 MHz, pD 7.4, 298 K) spectrum of **3** (7 mM). Proton assignments and NOE contacts are indicated with green lines; inter- and intramolecular cross peaks are marked with red squares.

suggesting the occurrence of an intermolecular contact within the self-assembled structure. A three-dimensional description of the trimer in solution was then attempted by combining molecular modelling calculations with the observed NMR data. Following the idea that hydrogen-bonding interactions between partially deprotonated phosphonates are the driving force for the self-assembly, several manual dockings of the trimer were built up and minimised as starting points for conformational searches. All but one of the designed structures resulted in unstable assemblies. The only stable trimer found (Figures 3 and S29) showed a structure composed of three monomer units, the first of which shows the cleft open outward, whereas the other two feature opposite naphthalene rings oriented perpendicularly to the first monomer unit. This assembly is held together by several hydrogen bonds between phosphonate groups (Figure 3a), reinforced by stacking interactions between aromatic units. This geometry explains the shielding effects observed on the H–C and CH_2 protons in that, if these protons belong to the second and the third monomer units, they are located over the carbazole moieties of the first unit (Figure 3c). In addition, the calculated structure also explains the NOE contact found between the H–C and H–D protons; indeed, it can be appreciated (Figure 3b) that the H–C protons of the first monomer unit point toward the H–D protons of the second unit, showing short interatomic distances.

Binding Studies

The binding properties of **3** were qualitatively investigated by ^{1}H-NMR spectroscopy in D_2O at pD 7.4 toward a set of monosaccharides (Scheme 2), including Neu5Ac, in addition to the α- and β-methyl glycosides of Glc, Gal, Man, GlcNAc, GalNAc, and Fuc, by monitoring the shifts of the proton signals of the sugar upon addition of an equimolar amount of **3** (Figure S10).

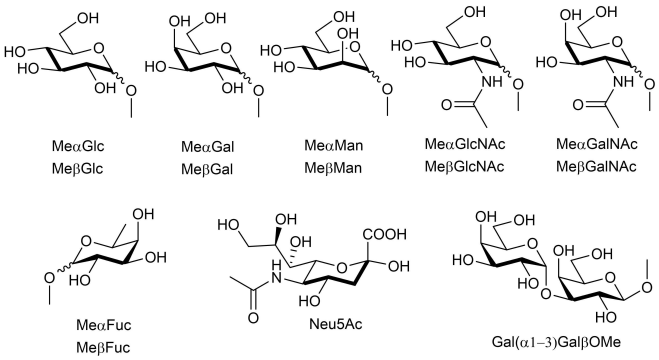

Scheme 2. Structures of the tested saccharides and their abbreviations.

Little ($\Delta\delta < 0.09$ ppm) or no changes were observed for Neu5Ac, MeβFuc, MeαGalNAc, MeβGalNAc, and MeαMan, whereas an appreciable upfield shift, together with broadening indicating slow chemical exchange, was observed for the rest of the set. However, the extent of the signal broadening changes within the set: it is modest for MeβGal, MeαFuc and MeαGlcNAc, is more pronounced for MeβMan and MeβGlcNAc, but leads to disappearance of most of the signals for MeαGlc, MeβGlc, and MeαGal, most likely due to strong binding.

A quantitative investigation by ^{1}H-NMR titrations in D_2O (pD 7.4, 298 K) was thus carried out on those monosaccharides that showed appreciable signal perturbation upon addition of **3**, additionally including the Gal(α1-3)GalβOMe disaccharide (Scheme 2). The trimerization constant was set invariant in the non-linear regression analysis of the receptor-glycoside binding data. The cumulative association constants, reported in Table 1, were measured simultaneously fitting the complexation induced shifts of all the available signals to the appropriate association model. Because multiple binding constants were measured, affinities were assessed through the intrinsic median binding concentration parameter BC_{50}^{0} [29] calculated from the

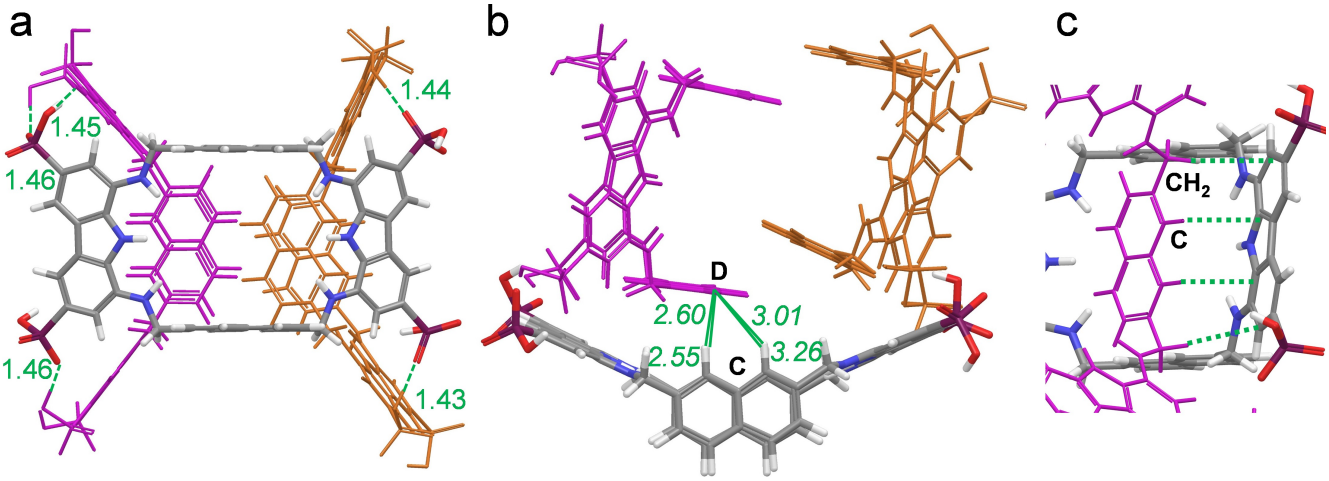

Figure 3. Global minimum of the trimeric structure of receptor **3**, in which the three monomer units are color-coded: the first in thick grey, the second in purple, the third in orange. a) Front view with intermolecular hydrogen-bonding interactions indicated as dashed lines, together with the corresponding oxygen/hydrogen distances [Å]; b) top view with intermolecular NOEs found between the H–C and H–D protons indicated as solid lines, with corresponding distances [Å]; c) side view showing interactions between naphthalene and carbazole moieties indicated as dotted lines.

Table 1. Cumulative formation constants ($\log\beta_n$)[a] and intrinsic median binding concentration (BC^0_{50}, [mM])[b] for receptor to glycoside (R:G) complexes of **3** with methyl glycosides, measured at 298 K from NMR and ITC data, in D_2O at pD 7.4 and in H_2O at pH 7.4, respectively.[c]

Glycoside	BC^0_{50}	log $\beta_{(3:1)}$	log $\beta_{(3:2)}$
MeαGlc	4.40 ± 0.54	9.61 ± 0.01	
MeβGlc	5.25 ± 0.65	9.52 ± 0.01	
MeαGal	1.91 ± 0.20	9.93 ± 0.03	12.24 ± 0.07
MeβGal	21.8 ± 3.02	8.87 ± 0.02	
MeβMan	9.57 ± 1.34	9.24 ± 0.03	
MeαGlcNAc	21.5 ± 3.42	8.87 ± 0.04	
MeβGlcNAc	13.1 ± 1.74	9.10 ± 0.01	
MeαFuc	27.8 ± 4.33	8.76 ± 0.04	
Gal(α1-3)GalβOMe	3.97 ± 0.54	9.66 ± 0.03	
Gal(α1-3)GalβOMe (ITC)	2.99 ± 0.35	9.80 ± 0.01	

[a] Formation constants were obtained by nonlinear least-square regression analysis of NMR and ITC data. [b] Calculated from the log β values using the "BC50 Calculator" program.[29] [c] Receptor trimerization constant ($\log\beta_{trim} = 6.71 \pm 0.06$) was set invariant in the nonlinear regression analysis of NMR and ITC data.

measured binding constants and reported in Table 1. Results show that receptor **3** maintains the ability of the parent receptor **1**, binding monosaccharides with affinities in the low millimolar range, in particular recognising axially substituted saccharides. The affinity order is in good agreement with the level of perturbation observed in the preliminary screening. Indeed, receptor **3** shows an affinity of 1.91 mM for the 1,4 disubstituted MeαGal, with a modest selectivity with respect to MeαGlc and MeβGlc, but more pronounced with respect to MeβMan and MeβGlcNAc by almost an order of magnitude. Interestingly, the lowest affinity was measured for MeαFuc, which, from the point of view of an achiral host as **3**, differs from MeαGal only for the hydroxylic group in position 6, suggesting a crucial role of this group in stabilizing the host-guest complex. The affinity of 9.57 mM for MeβMan is also noteworthy as, to the best of our knowledge, such an affinity for a mannoside in water has never been reported in the literature for a synthetic receptor.[32–35] However, the most remarkable result was recognition of the Gal(α1–3)GalβOMe disaccharide, which is bound with an unprecedented affinity of 3.97 mM, more than 2-fold larger than that observed for receptor **1** (9.18 mM), indicating that the tweezers-shaped architecture can better adapt to guests more complex than monosaccharides, as demonstrated by the open-chain receptor **2**.

The binding affinity observed toward Gal(α1-3)GalβOMe was further confirmed by ITC in H_2O at pH 7.4. Like for the NMR analysis, the measured trimerization constant was set invariant in the non-linear regression analysis of ITC data, which was performed by simultaneously fitting five independent titrations run at different reactant concentrations, in order to avoid ambiguities in the definition of the binding model. Cumulative binding constants, together with affinity value, were reported in Table 1 for Gal(α1-3)GalβOMe for a direct comparison with NMR results.

Unfortunately, because of the strong self-association of receptor **3**, ITC measurements did not provide reliable thermodynamic parameters.

Structure Studies of the Complex

To shed light on the binding mode of receptor **3** with mono- and disaccharides, a tridimensional description of the complex between MeαGal and Gal(α1-3)GalβOMe with **3** as a trimeric species was attempted using molecular modelling calculations supported by NMR data. The NOESY spectrum of a mixture of **3** and MeαGal (Figure 4a/b) showed unambiguous intermolecular NOE contacts between the glycosidic methyl and the H–C and H–D protons of the receptor, and between H-6 of the glycoside and protons H–D and H–E of the naphthalene moiety, clearly indicating a geometry in which the sugar is located between the two naphthalene rings. Interestingly, the NOESY spectrum also shows a contact between the H–C proton of the naphthalene and the H–A proton of the carbazole. Considering that the H–C and H–A protons are much too far apart in the structure of **3** to show an appreciable NOE effect, this cross peak has been more reasonably interpreted as an intermolecular contact related to the presence of the trimeric species of the receptor in solution. Because such a NOE contact was not observed in the NOESY spectra of receptor **3**, a slightly different arrangement of the trimer in the MeαGal complex is inferred. A NOESY spectrum carried out on a mixture of **3** and Gal(α1-3)GalβOMe (Figure 4c/d) showed intermolecular NOE contacts between the glycosidic methyl and H–D and H–E protons of the naphthalene, and between the H–E protons of the receptor and H-4 and H-5′ protons belonging to the two glycosidic units of the disaccharide. Because the latter protons are quite distant from the glycosidic methyl in the structure of the disaccharide, but all of them show NOE contacts with H–E, it is reasonable to ascribe these contacts to different monomer units of the trimer.

Conformational searches were carried out on the 3:1 complexes of **3** with MeαGal and Gal(α1-3)GalβOMe, starting from minimized structures in which the saccharides were manually docked into the most accessible cleft of the monomer unit. The calculation returned a single family of minimum energy conformers within 8.91 kJ mol^{-1} and 9.94 kJ mol^{-1} from the global minimum, respectively. The minimum energy structure for the complex between trimeric **3** and MeαGal, depicted in Figure 5a (and Figure S32), shows MeαGal located between the two naphthalene rings of a first monomer unit of the receptor, directing the methyl group across the macrocycle toward one of the naphthalene rings of a second monomer unit. The calculated structure was found to be in good agreement with the NOE contacts observed in the NOESY maps. As can be seen in Figure S33, recognition of MeαGal induces a tighter arrangment of the trimer, featuring a shortening of the relative distances between the H–A and H–D protons with respect to those of the uncomplexed trimer **3**. Whereas most of the proximities inferred from the NOE contacts were satisfied

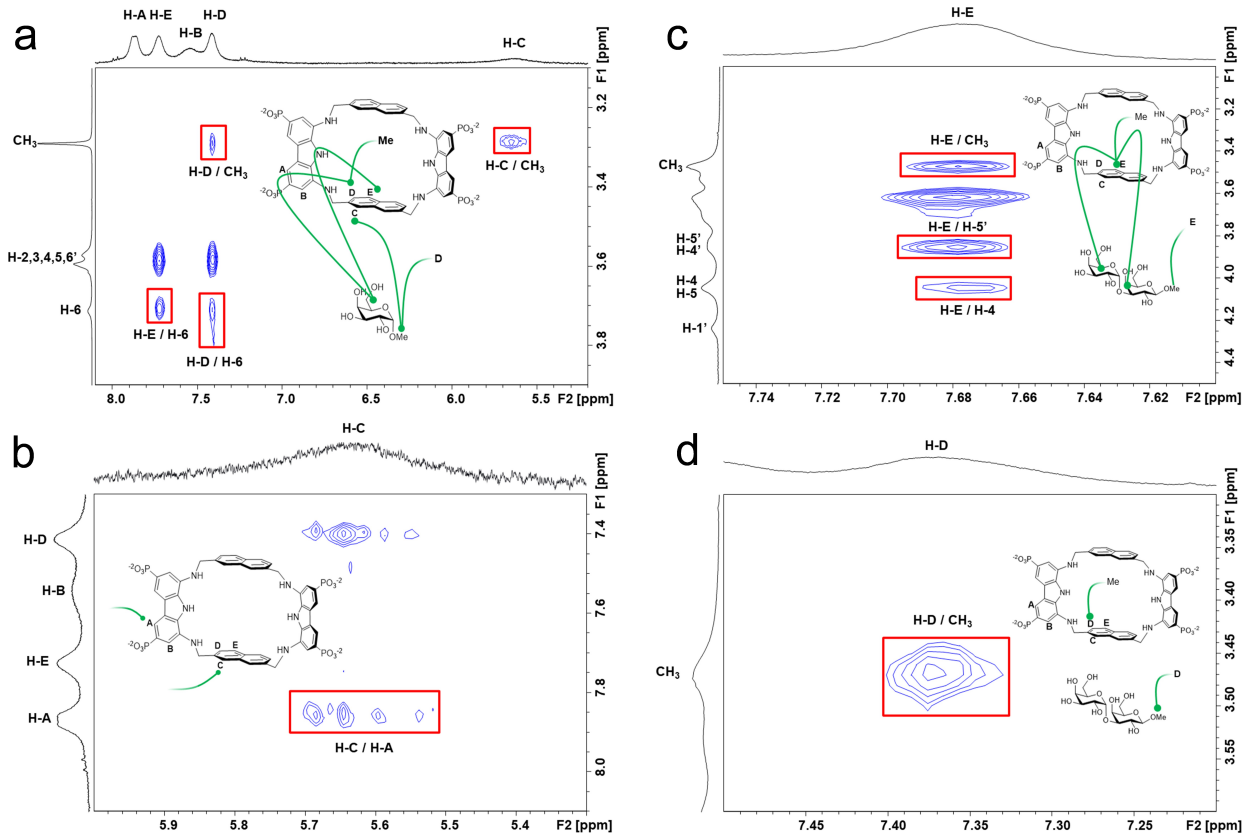

Figure 4. NOESY (800 ms mixing time, 500 MHz, pD 7.4, 298 K) spectra of: a) and b), **3** (2.5 mM) and MeαGal (7.5 mM); c) and d), **3** (7 mM) and Gal(α1-3)GalβOMe (21 mM). NOE contacts are indicated as green lines; intermolecular cross peaks are indicated in red squares.

by a single monomer unit of the receptor, the glycosidic methyl close to H–C but too far away from H–D of the same naphthalene was instead found close to the H–D proton of another monomer unit. In the binding cleft, the MeαGal features a disposition that maximises CH-π interactions with the two naphthalene rings and establishes several hydrogen bonds with diaminocarbazole moieties through oxygens in 1, 2 and 6 positions. In particular, H-6 is held in place by three hydrogen bonds, supporting the crucial role for binding of the OH-6 group, as suggested by the low affinity of MeαFuc, in which this group is missing.

A closely similar binding mode was found for the complex between **3** and Gal(α1-3)GalβOMe (Figure 5b and Figure S34) where, unexpectedly, the methyl β galactoside unit takes the place of MeαGal in the former complex, leaving the α galactoside unit mostly outside the binding cleft. A direct comparison of the geometries of the methyl galactoside units (α and β) within the binding site of the receptor (Figure S35) shows that, unlike for the β anomer, the α assumes a skewed geometry with respect to the naphthalene rings, to better accommodate both axial substituents and to maximise the CH-π interactions. The calculated structure is in agreement with the observed NOEs: indeed, whereas the H-4 and H-5′ protons are in proximity of the H–E protons of the first monomer unit of the receptor, the glycosidic methyl points toward a naphthalene ring of a second monomer unit, located in proximity of H–D and H–E of the latter. All O···H and N···H interatomic distances shorter than the sum of the van der Waals radii and compliant with hydrogen bonding criteria were calculated from the above model. A set of hydrogen-bonding interactions closely similar to those featured by the MeαGal complex were observed on the β galactoside unit but, interestingly, even though Gal(α1-3)GalβOMe is bound mainly through the β galactoside unit, the observed affinity is quite different from that of MeβGal. The larger affinity can most likely be ascribed to the additional hydrogen bond found between the OH-6 of the α galactoside unit and one of the amino groups of the receptor, indicating that both the galactoside units are involved in the recognition process.

A final comment is due to the recognition of the α-Gal epitope. We have shown that receptor **3** selectively binds to the Gal(α1-3)Galβ disaccharide; this does not guarantee that the actual epitope will be effectively recognized. However, we have shown that the cleft architecture of **2** selectively recognises *N*,*N*′-diacetylchitobiose (βGlcNAc$_2$), even when this is present in the core structure of N-glycans. Thus, it would not be surprising that the macrocyclic-cleft combination of **3** could indeed bind the entire trisaccharidic Gal(α1-3)Gal(β1-4)GlcNAc epitope. Because the glycosidic methyl group of the disaccharide appears to point to the macrocycle cavity, the additional GlcNAc unit may be located beyond the cavity, with the epitope treaded into the macrocycle, likely inducing a reorganization of the trimeric assembly. This hypothesis is suggested by preliminary

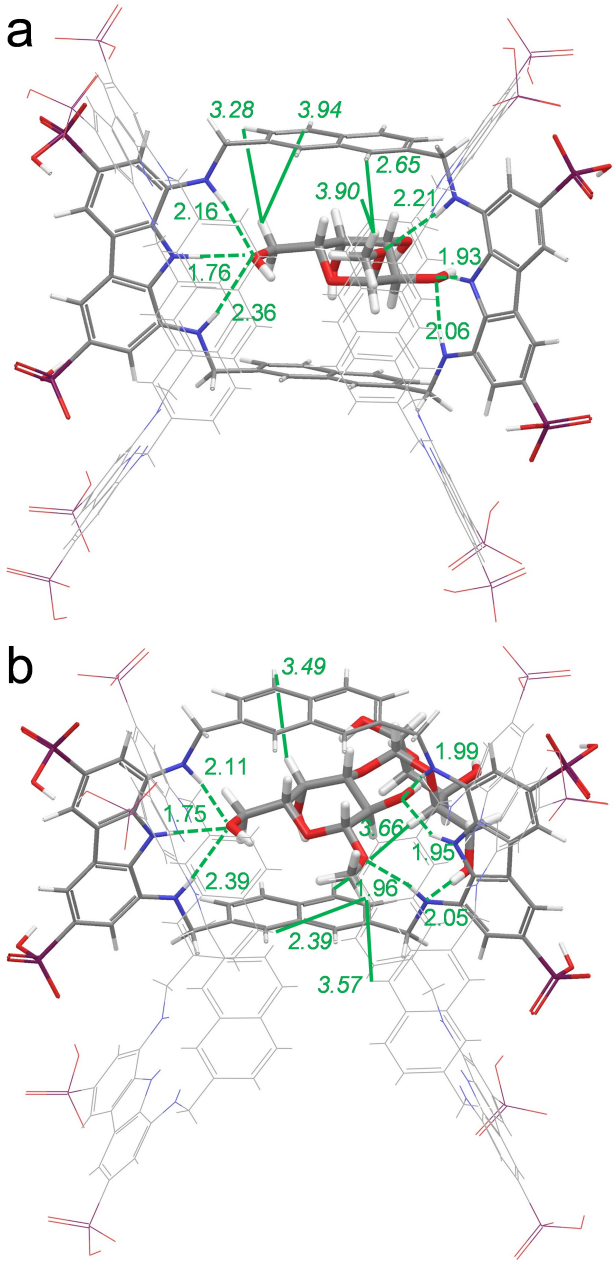

Figure 5. Global minimum structures of the 3:1 complexes of (a) **3**·MeαGal, and (b) **3**·Gal(α1-3)GalβOMe. The shortest intermolecular NOEs found are indicated as solid lines, with the corresponding distances [Å] calculated for the lowest energy conformer. Intermolecular hydrogen-bonding interactions found in the calculated structures are indicated as dashed lines, together with the corresponding oxygen/hydrogen and nitrogen/hydrogen distances [Å].

modelling calculations (Figure S32), showing a binding mode in which additional hydrogen bonds are established between the GlcNAc unit and the carbazole moiety.

Conclusions

In this work we have shown that combining the structural features of a macrocyclic architecture, binding axially-substituted monosaccharides, with a tweezers-like structure, tailored for disaccharides, is possible to obtain a new receptor capable of binding both mono- and disaccharides with distinct binding properties toward MeαGal and the Gal(α1-3)Gal disaccharide of the α-Gal antigen in the low millimolar range as assessed by NMR spectroscopy and confirmed by ITC measurements. The receptor can be easily prepared in high yield and shows a good selectivity for MeαGal over saccharides commonly found in glycan structures. The tweezers-like conformation of **3** accommodates the Gal(α1-3)GalβOMe disaccharide inside the binding cleft, where it is bound involving both the galactoside units. Because of the described binding properties, receptor **3** stands as an significant step forward in targeting saccharide epitopes of glycans with biomimetic receptors.

Supporting Information

The authors have cited additional references within the Supporting Information.[36–38]

Acknowledgements

The financial support provided by the MUR - Dipartimenti di Eccellenza 2023–2027 (DICUS 2.0) to the Department of Chemistry "Ugo Schiff" of the University of Florence is acknowledged. Ente Cassa di Risparmio di Firenze (Italy) is acknowledged for granting an ITC nanocalorimeter and a high-field NMR spectrometer. Open Access publishing facilitated by Università degli Studi di Firenze, as part of the Wiley - CRUI-CARE agreement.

Conflict of Interests

The authors declare no conflict of interest.

Data Availability Statement

The data that support the findings of this study are available in the supplementary material of this article.

Keywords: carbohydrates · α-gal epitope · host-guest · molecular recognition · synthetic receptors

[1] Y. van Kooyk, G. A. Rabinovich, *Nat. Immunol.* **2008**, *9*, 593–601.
[2] J. Y. Zhou, D. M. Oswald, K. D. Oliva, L. S. C. Kreisman, B. A. Cobb, *Trends Immunol.* **2018**, *39*, 523–535.
[3] S. S. Pinho, I. Alves, J. Gaifem, G. A. Rabinovich, *Cell. Mol. Immunol.* **2023**, *20*, 1101–1113.
[4] F. Milanesi, S. Roelens, O. Francesconi, *ChemPlusChem* **2023**, DOI 10.1002/cplu.202300598.
[5] O. Francesconi, S. Roelens, *ChemBioChem* **2019**, *20*, 1329–1346.
[6] B. A. Macher, U. Galili, *BBA-Gen. Subjects* **2008**, *1780*, 75–88.
[7] U. Galili, *Immunol. Cell Biol.* **2005**, *83*, 674–686.

[8] A. Cabezas-Cruz, A. Hodžić, P. Román-Carrasco, L. Mateos-Hernández, G. G. Duscher, D. K. Sinha, W. Hemmer, I. Swoboda, A. Estrada-Peña, J. de la Fuente, *Front. Immunol.* **2019**, *10*, DOI 10.3389/fimmu.2019.01210.
[9] U. Galili, *Front. Mol. Biosci.* **2021**, *8*, DOI 10.3389/fmolb.2021.746883.
[10] A. P. V. Moura, L. C. B. Santos, C. R. N. Brito, E. Valencia, C. Junqueira, A. A. P. Filho, M. R. V. Sant'Anna, N. F. Gontijo, D. C. Bartholomeu, R. T. Fujiwara, R. T. Gazzinelli, C. S. McKay, C. A. Sanhueza, M. G. Finn, A. F. Marques, *ACS Cent. Sci.* **2017**, *3*, DOI 10.1021/acscentsci.7b00311.
[11] A. Cabezas-Cruz, J. de la Fuente, *Front. Immunol.* **2017**, *8*, DOI 10.3389/fimmu.2017.01733.
[12] M. Gentili, C. Nativi, O. Francesconi, S. Roelens, *Carbohydr. Chem.* **2016**, *41*, 149–186.
[13] Z. Sun, B. Fan, M. J. Webber, *ChemSystemsChem* **2023**, *5*, DOI 10.1002/syst.202200050.
[14] H. Yao, H. Ke, X. Zhang, S. J. Pan, M. S. Li, L. P. Yang, G. Schreckenbach, W. Jiang, *J. Am. Chem. Soc.* **2018**, *140*, 13466–13477.
[15] S. Kubik, *Supramolecular Chemistry in Water*, Wiley-VCH, **2019**.
[16] A. P. Davis, *Chem. Soc. Rev.* **2020**, *49*, 2531–2545.
[17] C. Ke, H. Destecroix, M. P. Crump, A. P. Davis, *Nat. Chem.* **2012**, *4*, 718–723.
[18] W. Liu, Y. Tan, L. O. Jones, B. Song, Q.-H. Guo, L. Zhang, Y. Qiu, Y. Feng, X.-Y. Chen, G. C. Schatz, J. F. Stoddart, *J. Am. Chem. Soc.* **2021**, *143*, 15688–15700.
[19] P. Stewart, C. M. Renney, T. J. Mooibroek, S. Ferheen, A. P. Davis, *Chem. Commun.* **2018**, *54*, 8649–8652.
[20] X. Schaapkens, R. N. van Sluis, E. O. Bobylev, J. N. H. Reek, T. J. Mooibroek, *Chem. Eur. J.* **2021**, *27*, 13719–13724.
[21] T. S. Carter, T. J. Mooibroek, P. F. N. Stewart, M. P. Crump, M. C. Galan, A. P. Davis, *Angew. Chem. Int. Ed.* **2016**, *55*, 9311–9315.
[22] O. Francesconi, M. Martinucci, L. Badii, C. Nativi, S. Roelens, *Chem. Eur. J.* **2018**, *24*, 6828–6836.
[23] R. A. Tromans, S. K. Samanta, A. M. Chapman, A. P. Davis, *Chem. Sci.* **2020**, *11*, 3223–3227.
[24] S. Sharma, S. Shekhar, B. Sharma, P. Jain, *RSC Adv.* **2020**, *10*, 34099–34113.
[25] O. Francesconi, F. Cicero, C. Nativi, S. Roelens, *ChemPhysChem* **2020**, *21*, 257–262.
[26] O. Francesconi, F. Milanesi, C. Nativi, S. Roelens, *Chem. Eur. J.* **2021**, *27*, 10456–10460.
[27] F. Milanesi, L. Unione, A. Ardá, C. Nativi, J. Jiménez-Barbero, S. Roelens, O. Francesconi, *Chem. Eur. J.* **2023**, *29*, DOI 10.1002/chem.202203591.
[28] O. Francesconi, F. Milanesi, C. Nativi, S. Roelens, *Angew. Chem. Int. Ed.* **2021**, *60*, 11168–11172.
[29] A. Vacca, O. Francesconi, S. Roelens, *Chem. Rec.* **2012**, *12*, 544–566.
[30] V. Akhmetov, M. Feofanov, C. Ruppenstein, J. Lange, D. Sharapa, M. Krstić, F. Hampel, E. A. Kataev, K. Amsharov, *Chem. Eur. J.* **2022**, *28*, DOI 10.1002/chem.202200584.
[31] O. Francesconi, A. Ienco, F. Papi, M. Dolce, A. Catastini, C. Nativi, S. Roelens, *J. Org. Chem.* **2022**, *87*, 2662–2667.
[32] H. Abe, K. Okada, H. Makida, M. Inouye, *Org. Biomol. Chem.* **2012**, *10*, 6930–6936.
[33] O. Francesconi, C. Nativi, G. Gabrielli, M. Gentili, M. Palchetti, B. Bonora, S. Roelens, *Chem. Eur. J.* **2013**, *19*, 11742–11752.
[34] A. Ardá, C. Venturi, C. Nativi, O. Francesconi, F. J. Cañada, J. Jiménez-Barbero, S. Roelens, *Eur. J. Org. Chem.* **2010**, 64–71.
[35] M. F. Bravo, K. Palanichamy, M. A. Shlain, F. Schiro, Y. Naeem, M. Marianski, A. B. Braunschweig, *Chem. Eur. J.* **2020**, *26*, 11782–11795.
[36] A. Vacca, C. Nativi, M. Cacciarini, R. Pergoli, S. Roelens, *J. Am. Chem. Soc.* **2004**, *126*, 16456–16465.
[37] C. Frassineti, S. Ghelli, P. Gans, A. Sabatini, M. S. Moruzzi, A. Vacca, *Anal. Biochem.* **1995**, *231*. 374–382.
[38] P. Gans, A. Sabatini, A. Vacca, *J. Solution Chem.* **2008**, *37*, 467–476.

Manuscript received: May 6, 2024
Accepted manuscript online: May 31, 2024
Version of record online: July 11, 2024